Soft Matter

www.rsc.org/softmatter

Volume 9 | Number 40 | 28 October 2013 | Pages 9501–9728

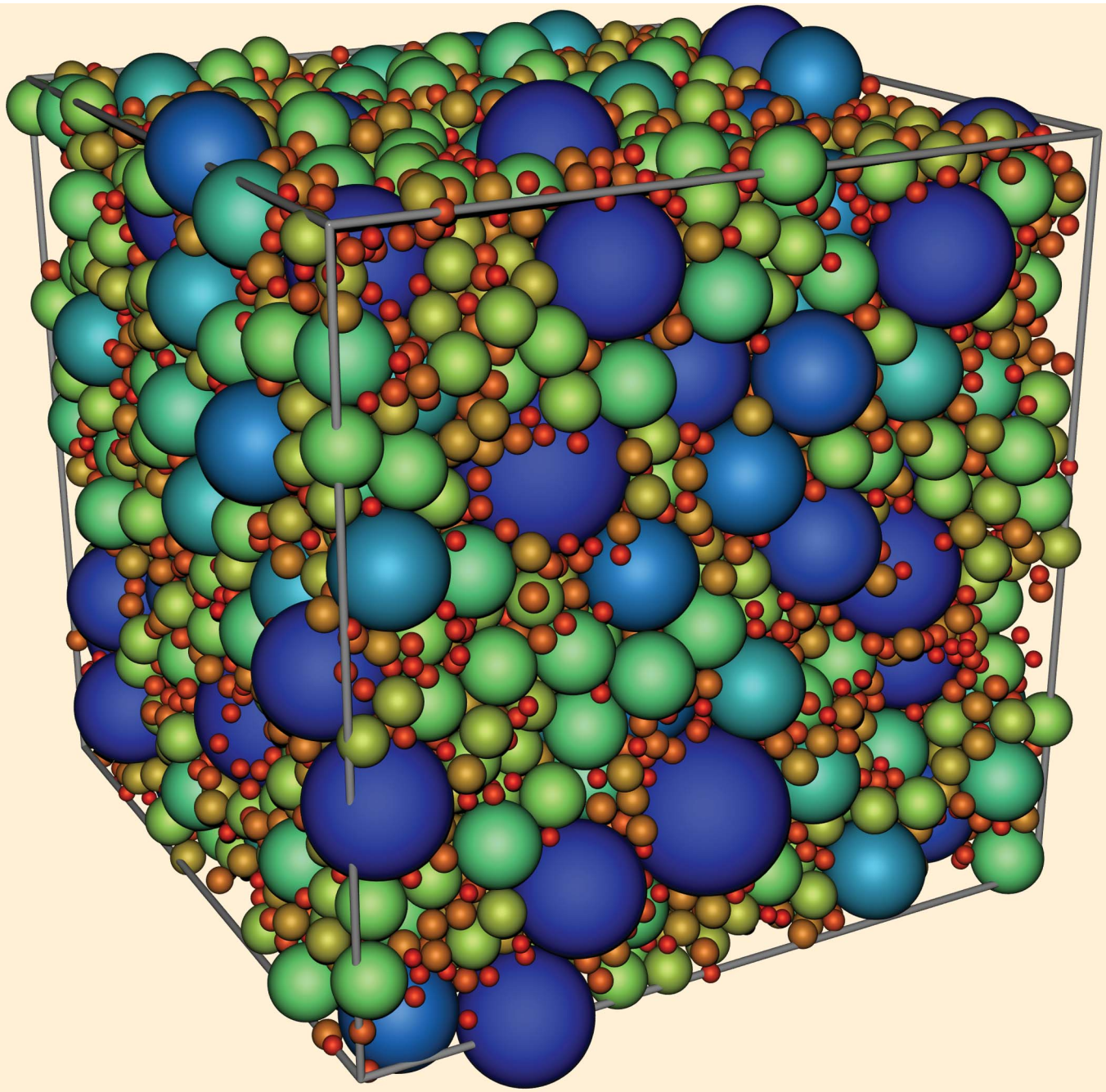

ISSN 1744-683X

RSC Publishing

COMMUNICATION

Vitaliy Ogarko and Stefan Luding

Prediction of polydisperse hard-sphere mixture behavior using tridisperse systems

Soft Matter

RSC Publishing

COMMUNICATION

Prediction of polydisperse hard-sphere mixture behavior using tridisperse systems†

Cite this: *Soft Matter*, 2013, **9**, 9530

Vitaliy Ogarko* and Stefan Luding

Received 8th April 2013
Accepted 18th July 2013

DOI: 10.1039/c3sm50964h

www.rsc.org/softmatter

How many state-variables are needed to predict the equation of state and the jamming density of polydisperse mixtures in glassy, non-equilibrium compressed states? We propose to define equivalent and maximally equivalent systems as those that match three and five moments of a given polydisperse size distribution, respectively. Fluids can be represented well by an equivalent system with only $s = 2$ components (bidisperse). As little as $s = 3$ components (tridisperse) are enough to achieve a maximally equivalent system. Those match macroscopic properties in glassy states, but also the volume fraction of rattlers, suggesting strong microstructural equivalency too. For many soft and granular systems, tridisperse, maximally equivalent systems allow for a closed analytical treatment and well-controlled industrial applications, while our proposal waits for experimental validation.

The hard-sphere model is one of the simplest representations of soft condensed matter systems where strong repulsions dominate the weak, or negligible attractive forces. It can be applied with some success for studying disorder–order transitions, the glass transition, colloids, granular materials, amorphous metals, and phase transitions or nucleation in simple gases and liquids.[1–4] Despite its simplicity, more complicated (soft) interactions of spheres can be approximated with the hard-sphere model.[5]

In many experimental or industrially relevant circumstances, the particular components (spheres) of a system are not uniform in size but rather display some distribution of sizes or "polydispersity".[6] Interesting phenomena arise in the presence of a wide polydispersity,[7] but due to the wide size distribution across many scales, it is difficult to provide simple accurate statistical models[8,9] for such systems. In many fluid-based theories, for example, Percus–Yevick integral equation theory,[10,11] scaled-particle theory,[12] Boublík, Mansoori, Carnahan, Starling, and Leland (BMCSL) equation of state (EOS),[13,14] Rosenfeld's fundamental measure theory,[15] A. Santos' approaches,[16–18] and others,[19–21] it is assumed that the dependence of the polydisperse pressure of N hard spheres on the $2N - 1$ degrees of freedom (volume fraction plus $N - 1$ size ratios and $N - 1$ independent mole fractions) can be encapsulated into the dependence of only three parameters, *i.e.*, the volume fraction and the second and third scaled moments (divided by the first moment, with the appropriate power). In this case, the equivalent mapping *polydisperse-to-bidisperse* is sufficient, because matching the first three moments of any radii distribution requires only two differently sized components. At the same time, the two-species kinetic theory is particularly simple, since two coupled equations for each species can be written down explicitly, whereas the multi-species theory is much less convenient.

A bidisperse equivalent mapping, while being very useful over a wide range of fluid volume fractions, $\nu_f \lesssim 0.56$, has limitations for extremely large densities in glassy, metastable states near the jamming transition. Equivalent bidisperse systems show (partial) crystallization for densities around ν_f already and, in general, do not perform well for $\nu > \nu_f$, due to the overwhelming presence of one species.[22] The *open question* is whether another mapping polydisperse-to-finite-number of components works, starting from as little as a three-component mixture.

We consider s-component mixtures of N_i hard spheres of radius a_i enclosed in a volume V, with $i = 1, \ldots, s$. In the case of a polydisperse size distribution, $s = N$ and each sampled a_i can be different from the others. The composition of such mixtures is quantified by the radii a_i and the partial volume fractions, $\nu_i = (4/3)\pi N_i a_i^3/V$, *i.e.*, one has $2s$ degrees of freedom (dof). The total volume fraction $\nu = \sum_1^s \nu_i$ and the arbitrary unit of length leave $2s - 2$ independent dof. We define *equivalent* systems as those that have the same first two scaled moments, $k = 2,3$, with $M_k = \langle a^k\rangle/\langle a\rangle^k$, with moments, $\langle a^k\rangle = \int a^k f(a)\mathrm{d}a$, of their normalized size distribution functions $f(a)$. Furthermore, *maximally equivalent* systems are those that have the same first four scaled

Multi Scale Mechanics (MSM), CTW, MESA+, University of Twente, PO Box 217, 7500 AE Enschede, the Netherlands. E-mail: v.ogarko@utwente.nl

† Electronic supplementary information (ESI) available. See DOI: 10.1039/c3sm50964h

This journal is © The Royal Society of Chemistry 2013

moments, $k = 2$–5, of their size distribution functions. Without loss of generality, it can be more convenient,†[20] to use central moments $\mu_k = \langle (a - \langle a \rangle)^k \rangle$.

The larger the s, the more moments of the size distribution can be adjusted, and due to more efficient packing it is possible to reach considerably higher jamming densities as compared to mono- or bidisperse cases. Perfectly space-filling (*e.g.*, Apollonian) packings are beyond the reach of tridisperse packings,[23] as well as infinitely slow routes to equilibrium states,‡ due to finite simulation times.

We perform event-driven molecular dynamics simulations using systems of hard spheres with periodic boundary conditions. Starting from zero volume fraction we compress the system towards a jammed state using a modification of the Lubachevsky–Stillinger algorithm,[25,26] which allows the diameter of the particles to grow linearly in time with a dimensionless rate Γ,§ while the kinetic energy, E, is kept constant using a re-scaling thermostat procedure.[22] An alternative growth method would decrease Γ with increasing density,[27] however, the used compaction process is well-defined nevertheless, and the resultant (non-equilibrium) states too – as confirmed by some different initial configurations – albeit subject to statistical fluctuation and ensemble averaging for small finite systems. The growth rate used in most simulations is slow, $\Gamma = 16 \times 10^{-6}$, if not explicitly stated otherwise. A few runs with ten times smaller Γ are consistent. The compressibility factor $Z \equiv pV/Nk_BT$ (dimensionless combination of pressure p and kinetic temperature $k_BT = 2E/3N$) is calculated from the total exchanged momentum in all interparticle collisions during a short time period. The following types of particle size distributions are used: (i) uniform size (rectangular); (ii) uniform volume, *i.e.*, the probability distribution of the volume of the particles is constant; (iii) tridisperse systems, equivalent to the aforementioned polydisperse systems. The considered polydisperse distributions are characterized by their width, *i.e.*, the ratio ω between the maximum and the minimum particle radius. (For details see the ESI,† where the log-normal distribution is also discussed.)

Our simulations confirm that in the fluid regime, *i.e.*, at volume fractions $\nu < 0.54$, the agreement in the compressibility factor Z between all considered systems and the BMCSL equation of state is better than 1% (data not shown).[22] When the density is further increased, the compressibility factor deviates from the fluid theory prediction that involves a maximum volume fraction of unity due to the density expansion involved, while the maximum solid volume fraction has to be lower due to the excluded volume. Z increases very rapidly at densities higher than the freezing point, so that we instead plot the estimated jamming density $\phi_J^{est}(\nu) = \nu/[1 - 3/Z(\nu)]$,[22] since it is limited, *i.e.*, $\phi_J^{est}(\nu) = \nu$ for $Z(\nu) \to \infty$. Fig. 1(a) shows ϕ_J^{est} as a function of volume fraction for a few systems with uniform size distribution (dark curves, *e.g.*, blue) and their tridisperse, maximally equivalent counterparts (light curves, *e.g.*, cyan), *i.e.*, with matched first four scaled moments. While for small size ratios, $\omega < 1.2$, ordering/crystallization is expected,†[22] for $1.2 \leq \omega \leq 3$ the estimated jamming density of the considered polydisperse systems and their respective tridisperse counterparts is in perfect agreement and still within 1% for the widest studied size distributions of width $\omega = 100$. We measured crystallinity¶ and found that maximally equivalent tridisperse systems do not show signs of crystallization for $\omega \geq 1.4$ (data are shown in the ESI†), while equivalent bidisperse systems partially crystallize for $\omega \gtrsim 5$, since then, the small particles fit into interstices and thus do not hinder crystallization of the large particles.[22] We also confirmed that systems with uniform volume distribution and their tridisperse maximal equivalents have close equations of state in the range $1.2 \leq \omega \leq 10$ (data not shown).

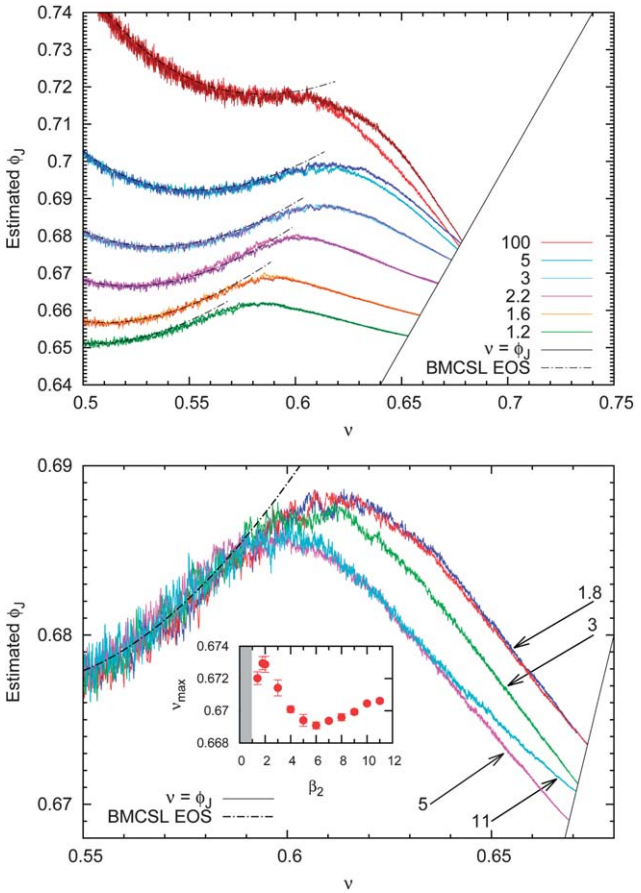

Fig. 1 Estimated jamming density, ϕ_J^{est}, plotted against volume fraction, ν, (a, top) for systems with $N = 4096$ and uniform size distribution (dark curves – dark green, dark orange-red, dark magenta, *etc.*) and their tridisperse maximal equivalents with the same N (light curves – green, orange-red, magenta, *etc.*), and (b, bottom) for the system with uniform size distribution with $\omega = 3$ (dark blue) and some tridisperse equivalents with different β_2. Given in the inset of (a) are the size ratios ω corresponding to curves with increasing ϕ_J^{est}. The values of β_2 in (b) are marked with arrows (for $\beta_2 = 1.8$ both tri- and polydisperse data are practically overlapping). In the inset of (b) the maximal reached volume fraction is plotted against the kurtosis β_2, where the error bars indicate the standard deviation of three different runs with random initial particle positions and velocities. The fluid theory (BMCSL EOS) is plotted as a dot-dashed line.

In Fig. 1(b) ϕ_J^{est} is plotted as a function of volume fraction for the uniformly polydisperse system with $\omega = 3$ (top curve) and its tridisperse equivalents. We fix the scaled moments $k = 2$, 3, 5‖ and vary the $k = 4$-moment, *i.e.*, the *kurtosis* $\beta_2 = \mu_4/{\mu_2}^2$, which describes both tailedness and peakedness of the size distribution function.[30] At high volume fractions, $\nu \geq \nu_F$, for glassy,

metastable states, the higher-order moments, *e.g.*, the kurtosis, play an important role. Even though the agreement is good for all equivalent systems with different β_2, it is close to perfect for the maximally equivalent system (with $\beta_2 = 1.8$), in both fluid and glassy regimes, including *almost* identical jamming densities.** In the inset of Fig. 1(b), the maximal reached volume fraction is plotted against the kurtosis β_2 (in general, $\beta_2 \geq 1$). The observed non-linear behavior can be explained by the vanishing presence of one species: for values of β_2 close to unity the system becomes nearly bidisperse due to vanishing concentration of the medium species, and for values of β_2 close to 12 the radius of the smallest species approaches zero (and becomes negative for $\beta_2 > 12$, so no physical solutions exist for this type of size distribution). Similar non-linear behavior of the jamming density was predicted and observed in ref. 32.

A small mismatch in jamming densities (such as with $Z > 10^{13}$) can be seen in Fig. 2(a), in the range $\omega \gtrsim 5$, where uniformly polydisperse systems jam at an about 0.5% higher density than their tridisperse maximal equivalents. We explain this deviation by linking the macro-scale jamming density with a micro-scale system property like "rattlers", *i.e.*, particles that are free to float in the cage made by their jammed neighbors. Due to particle growth (or, equivalently, compression of the system), the velocity of all particles increases at each collision.† Therefore, in denser situations, the velocity of the rattlers, which collide much less frequently, vanishes compared to the velocity of the jammed particles, due to the thermostat that simply rescales all velocities by the same factor.†† The simplest way to identify rattlers is to look at their speed, which is close to zero, whereas the scaled speed of jammed particles is close to unity. The rattler criterion is chosen as $v_r \leq 10^{-4}$ and we confirmed that changing the above criterion in the range $10^{-3} \leq v_r \leq 10^{-6}$ does not affect the results.

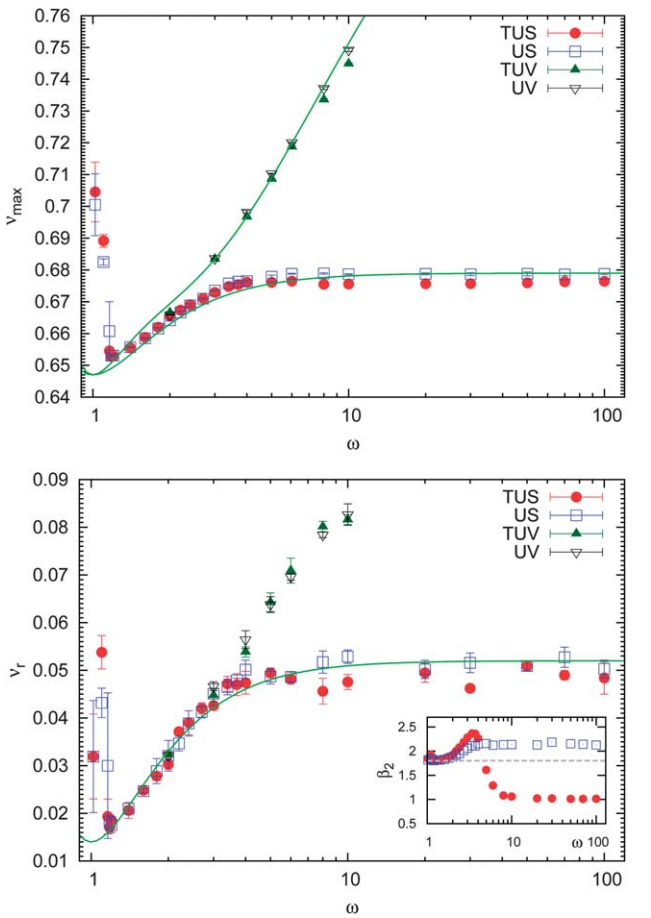

Fig. 2 (a, top) Jamming density plotted against ω for systems with uniform size (US, $N = 4096$) and uniform volume (UV, $N = 8192$) distributions and for their tridisperse maximal equivalents (TUS and TUV, respectively). Solid lines are fits from ref. 22 with parameters $\phi = 0.647$, $\nu_{us}^{\infty} = 0.679$ and $\nu_{uv}^{\infty} = 0.86$. (b, bottom) Volume fraction ν_r of rattlers plotted against ω for systems considered in (a). The solid line is the same fitting function as in (a) for the US data, but with different parameters $\phi = 0.014$ and $\nu_r^{\infty} = 0.052$. The error bars indicate the standard deviation of three different runs with random initial particle positions and velocities. The kurtosis of the US/TUS systems is plotted in the inset with rattlers ($\beta_2 = 1.8$, dashed line) and with rattlers excluded (symbols).

Fig. 2(b) shows the volume fraction of rattlers ν_r for many different size ratios, for the uniform size and uniform volume distributions and for their tridisperse maximal equivalents. Surprisingly, for $\omega \geq 1.2$, ν_r is very similar for poly- and the respective tridisperse systems. This shows that the maximal equivalent systems also have a very similar microstructure in that respect. (We also found that the poly- and the respective tridisperse structure factors have very similar low-wavenumber behavior).† Moreover, ν_r correlates with the jamming density in Fig. 2(a), *i.e.*, larger ν_{max} correlates with larger ν_r. Interestingly, ν_r for the US/TUS systems is described by the same functional form as the jamming density in Fig. 2(a). Note that when rattlers are excluded, the size distributions are not equivalent anymore, as quantified by the kurtosis in the inset of Fig. 2(b). The kurtosis considering non-rattlers only deviates from $\beta_2 = 1.8$ for both systems already for $\omega > 2$. The tridisperse and polydisperse data develop differently from each other at $\omega \gtrsim 4$, and reach plateaus for $\omega \geq 10$. In the TUS system, number fractions n_i change from their original values (with rattlers) 5 : 8 : 5 to 0 : 5 : 5, *i.e.*, all small particles and about 40% of the medium particles become rattlers. The strong decrease of β_2 for the tridisperse systems (in contrast to a small increase for the polydisperse systems) explains the small but systematic differences between their ν_{max}-values for $\omega \gtrsim 4$. The non-rattlers form the jammed system[33] and their size distribution (and moments) are relevant for the jamming density. In other words, tridisperse systems are equivalent to polydisperse systems if the size distribution moments of the fraction of non-rattlers are matched. *A priori* this was impossible, but observations that (i) the volume fractions of rattlers are almost identical and (ii) ν_r has the same functional form as the jamming density (for the US/TUS systems at least) provide a first step towards truly maximally equivalent tridisperse systems.

In conclusion, starting from different polydisperse systems, we defined equivalent and maximally equivalent hard sphere systems on the basis of identical first two and four scaled moments of their size distribution functions, respectively. By means of event-driven molecular dynamics simulations we confirmed that equivalent (bidisperse) systems match and predict the behavior of the polydisperse system in the fluid regime. Interestingly, maximally equivalent tridisperse systems

This journal is © The Royal Society of Chemistry 2013

match/predict polydisperse ones for much higher densities – in non-equilibrium, glassy states. Tridisperse systems do not suffer from partial crystallization, as observed for large size ratios in equivalent bidisperse systems,[22] and even allow prediction of the maximal jamming density within about 0.5% accuracy.

We identified the rattlers in glassy systems as the reason for this small but significant discrepancy. The size distributions of poly- and (maximally equivalent) tri-disperse systems with rattlers excluded are considerably different from the original one and from each other, as quantified by the kurtosis. The maximally equivalent tridisperse systems have almost the same volume fraction of rattlers as the polydisperse ones they mimic, which indicates a very strong similarity in the microstructures, with respect to caging, percolation, and volume fraction of non-rattlers. *Thus, truly maximally equivalent systems are those with four identical scaled moments of the non-rattlers*.

Important consequences of our research are: (i) a tridisperse theory is still analytically treatable (like for bidisperse systems, without further assumptions), whereas an arbitrary polydispersity would require arbitrarily many species and coupled equations; (ii) other transport coefficients (like heat-conductivity, viscosity *etc.*) can be computed analytically in the framework of a tridisperse theory (which goes beyond the scope of this study) and it should be checked if the 4-moments equivalency postulate holds for them too; (iii) experimentally, three species are much easier to control and (according to our prediction) should resemble multi-disperse systems; (iv) the multi-scale nature of wide polydispersities (continuous from very small to very large sizes) could be replaced by a discrete (three-scales only) picture (model system) that covers a narrower range of particle sizes – thus representing a working multi-scale theory with enormous reduction of complexity.

In future studies, the effect of the growth rate and especially the limit $\Gamma \to 0$ should be studied further and a comparison with experiments should be carried out with the goal to validate the present theoretical predictions and establish their relevance in the presence of more realistic contact interactions like friction.

The authors would like to thank A. Santos, N. Brilliantov, R. P. Behringer, E. Clément, S. Torquato, and N. Rivas for helpful discussions. This research is supported by the Dutch Technology Foundation STW, which is the applied science division of NWO, and the Technology Programme of the Ministry of Economic Affairs, project Nr. STW-MUST 10120.

Notes and references

‡ Thermodynamically, the polydisperse system fractionates in phases separated according to the particle size, but this eutectic freezing-transition is kinetically suppressed and practically unreachable.[24]

§ The growth rate is defined as $\Gamma = \frac{\mathrm{d}a_i}{\mathrm{d}t}\frac{a_{\max}}{a_i}\sqrt{\frac{3M}{2E}}$, with the largest particle radius, $a_{\max}$, and total system mass, M.

¶ Particles in a crystalline environment were identified using a method based on spherical harmonics given in ref. 28; the bond network was determined using a weighted Delaunay tessellation,[29] effectively taking into account the strongly different radii of the particles.

‖ $\mu_5 \equiv 0$ for the uniform size distribution.

** The importance of the fourth and fifth moments is also supported by estimates for the contact number density of static, soft granular packings, see ref. 31 and references therein.

†† With this thermostat, the jammed network of non-rattlers equilibrates itself, while the rattlers are artificially "cooled" down. Alternative thermostats would "heat" rattlers without changing the system behavior since those would still collide much less than the jammed non-rattlers due to their larger mean free path.

1 S. Chapman and T. G. Cowling, *The mathematical theory of nonuniform gases*, Cambridge University Press, London, 1960.
2 J. M. Ziman, *Models of Disorder*, Cambridge University Press, Cambridge, 1979.
3 J. P. Hansen and I. R. McDonald, *Theory of simple liquids*, Academic Press Limited, London, 1986.
4 *Granular Gases*, ed. T. Pöschel and S. Luding, Springer, Berlin, 2001.
5 N. Xu, T. K. Haxton, A. J. Liu and S. R. Nagel, *Phys. Rev. Lett.*, 2009, **103**(24), 245701; M. Schmiedeberg, T. K. Haxton, S. R. Nagel and A. J. Liu, *EPL*, 2011, **96**(3), 36010.
6 M. Clusel, E. I. Corwin, A. O. N. Siemens and J. Brujic, *Nature*, 2009, **460**(7255), 611–615.
7 M. A. Bates and D. Frenkel, *J. Chem. Phys.*, 1998, **109**, 6193; P. N. Pusey and W. van Megen, *Nature*, 1986, **320**, 340; R. M. L. Evans, D. J. Fairhurst and W. C. K. Poon, *Phys. Rev. Lett.*, 1998, **81**, 1326.
8 K. Gotoh and J. L. Finney, *Nature*, 1974, **252**, 202–205.
9 E. I. Corwin, M. Clusel, A. O. N. Siemens and J. Brujic, *Soft Matter*, 2010, **6**(13), 2949–2959.
10 J. K. Percus and G. J. Jevick, *Phys. Rev.*, 1958, **110**, 1.
11 J. L. Lebowitz, *Phys. Rev.*, 1964, **133**, A895.
12 H. Reiss, H. L. Frisch, E. Helfand and J. L. Lebowitz, *J. Chem. Phys.*, 1960, **32**, 119.
13 T. Boublík, *J. Chem. Phys.*, 1970, **53**(1), 471.
14 G. Mansoori, N. Carnahan, K. Starling and T. Leland, *J. Chem. Phys.*, 1971, **54**(4), 1523–1525.
15 Y. Rosenfeld, *Phys. Rev. Lett.*, 1989, **63**, 980–983.
16 A. Santos, S. Yuste and M. de Haro, *J. Chem. Phys.*, 2005, **123**(23), 234512.
17 A. Santos, *J. Chem. Phys.*, 2012, **136**(13), 136102.
18 M. López de Haro, S. Yuste and A. Santos, in *Theory and Simulation of Hard-Sphere Fluids and Related Systems*, ed. N. Mulero, Springer, Berlin/Heidelberg, Lecture Notes in Physics, 2008, vol. 753, pp. 183–245.
19 P. Bartlett, *J. Chem. Phys.*, 1997, **107**(1), 188–196.
20 P. Bartlett, *Mol. Phys.*, 1999, **97**(5), 685–693.
21 M. Fasolo and P. Sollich, *Phys. Rev. Lett.*, 2003, **91**(6), 068301.
22 V. Ogarko and S. Luding, *J. Chem. Phys.*, 2012, **136**(12), 124508.
23 R. M. Baram, H. J. Herrmann and N. Rivier, *Phys. Rev. Lett.*, 2004, **92**(4), 044301.
24 A. Donev, F. H. Stillinger and S. Torquato, *J. Chem. Phys.*, 2007, **127**(12), 124509.
25 B. D. Lubachevsky and F. H. Stillinger, *J. Stat. Phys.*, 1990, **60**(5/6), 561–583.
26 A. Donev, S. Torquato and F. H. Stillinger, *J. Comput. Phys.*, 2005, **202**(2), 737–764.
27 L. V. Woodcock, *J. Phys. Chem. B*, 2012, **116**(12), 3735–3744.

28 P. R. ten Wolde, M. J. Ruiz-Montero and D. Frenkel, *Faraday Discuss.*, 1996, **104**, 93–110.
29 L. Pournin, On the behavior of spherical and non-spherical grain assemblies, its modeling and numerical simulation, Ph.D. thesis, École Polytechnique Fédérale de Lausanne, 2005.
30 L. T. DeCarlo, *Psychol. Meth.*, 1997, **2**, 292–307.
31 M. R. Shaebani, M. Madadi, S. Luding and D. E. Wolf, *Phys. Rev. E: Stat., Nonlinear, Soft Matter Phys.*, 2012, **85**, 011301.
32 R. S. Farr and R. D. Groot, *J. Chem. Phys.*, 2009, **131**, 244104.
33 D. Bi, J. Zhang, B. Chakraborty and R. P. Behringer, *Nature*, 2011, **7377**, 355–358.

This journal is © The Royal Society of Chemistry 2013